Ground state of the random-bond spin-1 Heisenberg chain

Sara Bergkvist,* Patrik Henelius, and Anders Rosengren

Condensed Matter Theory,Physics Department, KTH, SE-106 91 Stockholm, Sweden

(Dated: February 1, 2008)

Stochastic series expansion quantum Monte Carlo is used to study the ground state of the antiferromagnetic spin-1 Heisenberg chain with bond disorder. Typical spin- and string-correlations functions behave in accordance with real-space renormalization group predictions for the random-singlet phase. The average string-correlation function decays algebraically with an exponent of -0.378(6), in very good agreement with the prediction of $-(3-\sqrt{5})/2 \simeq -0.382$, while the average spin-correlation function is found to decay with an exponent of about -1, quite different from the expected value of -2. By implementing the concept of directed loops for the spin-1 chain we show that autocorrelation times can be reduced by up to two orders of magnitude.

I. INTRODUCTION

The ground state of quantum spin chains displays a rich variety of physical phenomena such as quasi-long-range order, quantum phase transitions and hidden order parameters. Some models are exactly solvable by Bethe ansatz techniques, while others have to be approached using approximate techniques such as spin-wave theory, renormalization group (RG) methods, bosonization or numerical simulations.[1] Some methods, such as the density matrix renormalization group technique,[2] have been developed in the context of spin chains.

The introduction of disorder into quantum spin chains appears to create a very complex problem, yet there has been remarkable success in understanding and solving certain strongly disordered spin chains. Using a real-space renormalization group method Ma, Dasgupta and Hu were able to obtain many results for the bond-disordered spin-1/2 Heisenberg chain.[3] Fisher managed to solve the RG equations exactly for the spin-1/2 case,[4] and he showed that the ground state is the so-called random-singlet phase, where all spins pair up and form singlets over arbitrarily large distances. The characteristic time scale is an exponential function of the length scale, resulting in a dynamic critical exponent $z = \infty$. The random-singlet phase is gapless and average correlation functions decay algebraically, while typical correlations decay exponentially. Due to the singlet coupling between spins the decay exponents are predicted to be equal for all components of the correlation function, even if the Hamiltonian is anisotropic. In the RG calculation any initial randomness flows to the infinite-disorder random-singlet fixed point. Many of these striking prediction have been confirmed by numerical studies.[5,6,7,8]

The physics of the clean spin-1 chain is dramatically different from the spin-1/2 chain due to the presence of the Haldane gap,[9] accompanied by exponentially decreasing spin-correlation functions and a non-zero string-order parameter. The effects of adding disorder to the spin-1 chain are more controversial, since the RG equations cannot be solved analytically in this case. By mapping the spin-1 chain to an effective spin-1/2 system Hyman and Yang argue that the spin-1 chain is stable against weak disorder,[10] but for a sufficiently strong disorder the chain undergoes a second order phase transition to the random-singlet phase. A density matrix renormalization group study finds no evidence of such a transition,[11] but Hyman and Yang suggest that the disorder was not strong enough in the numerical study.[12] However, for the same disorder distribution a recent quantum Monte Carlo (QMC) study finds evidence of a transition to the random-singlet phase,[13] and a new RG study also supports this result.[14]

In a further attempt to resolve the nature of the ground state of the strongly disordered spin-1 chain our goal is to study the average and typical spin- and string-correlation functions. The decay and distribution of these functions is one of the hallmarks of the random-singlet phase, and has been studied numerically to confirm the random-singlet picture for the spin-1/2 chain.[5,7,8] To obtain this goal we perform QMC simulations at a temperature low enough so that the observables in question have obtained their ground state expectation values. We use the stochastic series expansion QMC algorithm[15] in our calculations, and by applying the recently introduced concept of directed loops[16] to the spin-1 chain we demonstrate that autocorrelation times can be decreased by up to two orders of magnitude in the cases we have examined.

The outline of the paper is as follows: in Sec. II we review the basics of the stochastic series expansion. In Sec. III we implement the method of directed loops for the spin-1 case, and show the effects on the autocorrelation times. The method used to determine average and typical correlations is discussed in Sec. IV. Results for the ground state behavior of the random-bond spin-1 chain are shown in Sec. V. We conclude with summary and discussion in Sec. VI.

II. OPERATOR-LOOP ALGORITHM

The stochastic series expansion is described in detail elsewhere.[15] In this section we give a brief summary in

order to explain the new features we introduce in Sec. III.

The model treated in this article is the one-dimensional antiferromagnet spin-1 Heisenberg chain with bond disorder. The Hamiltonian, H, is given by,

$$H = \sum_i J_i \mathbf{S}_i \cdot \mathbf{S}_{i+1}, \tag{1}$$

where $\mathbf{S}$ denotes a spin-1 operator and the positive coupling parameter J_i, is randomly distributed.

The partition function, Z, is Taylor expanded,

$$Z = \sum_\alpha \sum_{m=0}^\infty \frac{(-\beta)^m}{m!} \langle \alpha | H^m | \alpha \rangle, \tag{2}$$

in the basis $\{|\alpha\rangle\} = \{|S_1^z, S_2^z, .., S_N^z\rangle\}$, where N is the number of spins. The inverse temperature is denoted by β.

Next we rewrite the Hamiltonian as a sum over diagonal and off-diagonal operators,

$$H = -\sum_{b=1}^N J_b (H_{1,b} - H_{2,b}), \tag{3}$$

where N is the number of spins and b denotes a bond corresponding to a pair of interacting spins $j(b)$ and $k(b)$. The operators are given by

$$
\begin{aligned}
H_{1,b} &= C - S_{j(b)}^z S_{k(b)}^z \\
H_{2,b} &= \frac{1}{2}(S_{j(b)}^+ S_{k(b)}^- + S_{j(b)}^- S_{k(b)}^+),
\end{aligned}
\tag{4}
$$

where C is a constant inserted to assure that the weight function is positive for all configurations.

To simplify the Monte Carlo update we introduce an additional unit operator $H_{0,0} = 1$. Inserting the Hamiltonian given by Eq. (3) into Eq. (2), and truncating the sum at $m = L$ we obtain

$$Z = \sum_\alpha \sum_{S_L} \frac{\beta^n (L-n)!}{L!} \langle \alpha | \prod_{i=1}^L J_{b_i} H_{a_i, b_i} | \alpha \rangle, \tag{5}$$

where S_L denotes a sequence of operator-indices

$$S_L = (a_1, b_1)_1, (a_2, b_2)_2, ..., (a_L, b_L)_L, \tag{6}$$

with $a_i = 1, 2$ and $b_i = 1, \ldots, N$ or $(a_i, b_i) = (0,0)$ and n is the number of non-unit operators in S_L.

The Monte Carlo procedure must hence sample the space of all states $|\alpha\rangle$, and all sequences S_L. The simulation starts with some random state $|\alpha\rangle$ and an operator string containing only unit operators. One Monte Carlo step consists of a diagonal and an off-diagonal update. In the diagonal update attempts are made to exchange unit and diagonal operators sequentially at each position in the operator string. Defining the propagated state

$$|\alpha(p)\rangle \sim \prod_{i=1}^p H_{a_i, b_i} |\alpha\rangle, \tag{7}$$

the probability for inserting or deleting a diagonal operator at place p in the operator string is given by detailed balance,[15]

$$P([0,0]_p \to [1,b]_p) = \frac{J_b N \beta \langle \alpha(p-1)|H_{1,b}|\alpha(p-1)\rangle}{L - n} \tag{8}$$

$$P([1,b]_p \to [0,0]_p) = \frac{L - n + 1}{J_b N \beta \langle \alpha(p-1)|H_{1,b}|\alpha(p-1)\rangle}.$$

The inclusion of J_b in the expressions above represents the place where the bond disorder appears explicitly in the algorithm. Removing or inserting an operator changes the expansion power n by ± 1.

The off-diagonal update, also called loop update, is carried out with n fixed. Each bond operator $H_{b_i} = H_{1,b_i} + H_{2,b_i}$ acts only on two spins, $S_{j(b_i)}$ and $S_{k(b_i)}$. We can therefore rewrite the matrix elements in Eq. (5) as a product of n terms, called vertices,

$$M(\alpha, S_L) = \prod_{i=1}^n W_{v(i)}, \tag{9}$$

where the vertex weight $W_{v(i)}$ is defined as

$$
\begin{aligned}
W_{v(i)} = \\
\langle S_{j(b)}^z(p) S_{k(b)}^z(p) | H_{b_i} | S_{j(b)}^z(p-1) S_{k(b)}^z(p-1) \rangle.
\end{aligned}
\tag{10}
$$

A vertex thus consists of four spins, called the legs of the vertex, and an operator.

The principles of the loop update are: one of the n vertices is chosen at random and one of its four legs is randomly selected as the entrance leg. The entrance leg is given a random state that differs from its initial state. One of its four legs is chosen as the exit leg, and its state is also changed. In order to satisfy detailed balance the exit leg is chosen with a probability proportional to the vertex weight $W_{v(i)}$ after the spins have been flipped. Thereafter the vertex list is sequentially searched for the next vertex that contains the exit spin. This spin becomes the entrance leg of the next vertex and this procedure is continued until the loop reaches the original entrance leg, when the loop closes. During one Monte Carlo step the loop update is repeated until on average all the vertices have been updated.

III. DIRECTED LOOPS FOR SPIN-1 CHAIN

The operator-loop formulation described above is applicable to a wide variety of models.[17] The efficiency of the algorithm does, however, depend on the model in question. It is particularly efficient for cases where the so-called bounce or backtrack process can be avoided. If the entrance and exit legs of a vertex coincide, the vertex spin configuration is left unchanged and the loop backtracks to the previous vertex. This is undesirable since the bounce process does not achieve any change in the SSE configuration. For models such as the spin-1/2 Heisenberg model and spin-1/2 XX model, where the

bounce process can be avoided, the autocorrelation times are generally significantly shorter than for cases where the bounce has to be included.

Recently Sandvik and Syljuåsen showed that, by introducing the notion of directed loops, it is possible to exclude the bounce process for a spin-1/2 chain in a wide parameter regime.[16] The application to more general models is also discussed in Ref. 16, as well as in Ref. 18. We will now show in some detail how the bounce process can be eliminated also for the spin-1 case.

The detailed balance principle requires that the probabilities of changing between two state, s and s', with weight functions $W(s)$ and $W(s')$, satisfy

$$W(s)P(s \rightarrow s') = W(s')P(s' \rightarrow s). \quad (11)$$

By considering all possible loop configurations that take us from configuration s to s', as well as the "time"-reversed paths returning to configuration s, Sandvik and Syljuåsen showed that the detailed balance criteria is satisfied if the local vertex condition

$$W_s P(s, l_1 \rightarrow s', l_2) = W_{s'} P(s', l_2 \rightarrow s, l_1) \quad (12)$$

is fulfilled. W_s denotes the vertex weight, given by Eq. (10), and $P(s, l_1 \rightarrow s', l_2)$ is the probability to choose exit leg l_2, given entrance leg l_1. The spin configuration of the vertex changes from s to s'. This criteria relates the transfer probabilities of two processes where the direction of the loop segment is reversed, since the entrance and exit legs are interchanged. Considering that the probabilities for choosing different exit legs should sum to unity Eq. (12) immediately leads to

$$W_s = \sum_{l_2} W_s P(s, l_1 \rightarrow s', l_2). \quad (13)$$

We can use Eq. (12) and Eq. (13) to construct the probabilities, $P(s, l_1 \rightarrow s', l_2)$, needed to perform the loop update. It turns out that it is possible to divide the space of all processes into subspaces, where only vertices in the same group are related to each other by Eq. (12). Hence, one may solve the detailed balance equations for each transformation group separately, and in many cases it is possible to find a solution with no bounce processes.

We now show how to apply this method to the spin-1 chain, and how to solve the resulting equations in a manner that eliminates the bounce process also in this case. For the spin-1 model there are in total 52 transformation groups, but many of them can be transformed into each other by symmetry arguments. There are five irreducible groups with two vertices, two groups with three elements, and one group with four vertices. The last group is shown in Fig. 1, where the operator of each vertex is shown as a horizontal line. The operator acts on the two spins above it, resulting in the spin configuration shown below it. Each row represent all vertices that can be reached from a given entrance leg with a given spin projection. Eq. (13) gives us the following set of equations
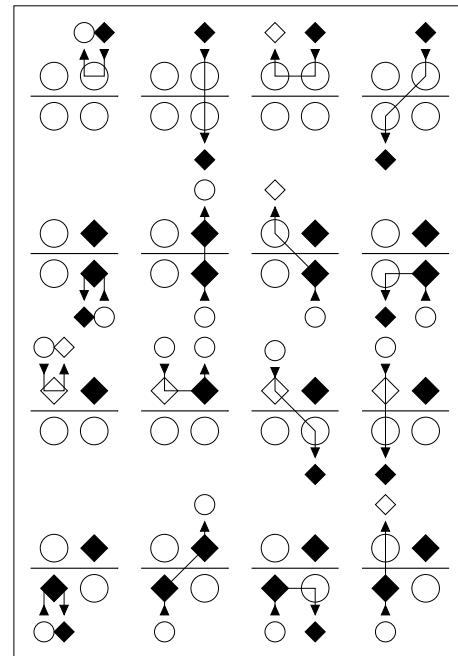
$$W_1 = a_1 + b + c + d \quad (14)$$

FIG. 1: An example of a transformation group with four vertices. The solid (empty) diamonds represent a spin projection of +1 (-1), and the circles the projection of 0. The lines with arrows are the directed loop segments. A row in the figure shows all possible updates of the vertex for a given entrance leg and spin state. The smaller symbols at the beginning and end of the loop segment show the entrace and exit spin states after the update.

$$W_2 = a_2 + b + e + f$$
$$W_3 = a_3 + c + e + g$$
$$W_4 = a_4 + d + f + g.$$

The weight on the left-hand side refers to the weight of the bare vertex, given by Eq. (10), while the weights on the right-hand side refer to the product of vertex weight and the transfer probability. Processes that are related to each other by changing the direction of the loop segment, and interchanging spin configurations, are given equal weights, according to Eq. (12). It is possible to solve this set of equations under the restriction that all bounce processes a_i are zero. There is not a unique solution since the number of unknowns exceeds the number of equations, and we have chosen the solution which gives all the allowed vertices equal weight.

For the spin-1 case the groups can be classified according to the change in spin projection on the entrance spin. All the groups where the spin projection changes by one can be solved so that the bounce is eliminated. There are, however, also four groups where the spin projection changes by two, shown in Fig. 2. The bounce cannot be eliminated in this case. The equations for the group in the bottom right corner are of the form
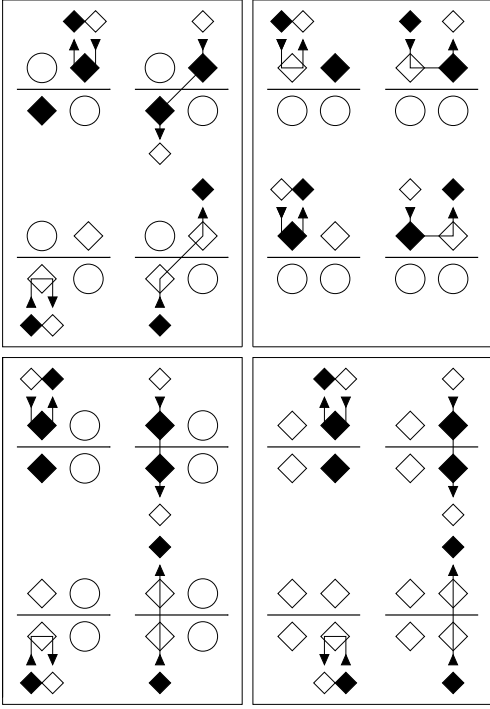
$$W_1 = a_1 + b = C + 1 \quad (15)$$

FIG. 2: The four transformation groups for the spin-1 chain, in which the magnetization changes by two. The solid (empty) diamonds represent a spin projection of +1 (-1), and the circles a projection of 0.

$$W_2 \;=\; a_2 + b = C - 1,$$

and the bounce processes a_1 and a_2 cannot be eliminated. We can, however, solve all groups shown in Fig. 2 so that the *only* processes allowed are the bounces. This means that any attempt to change the magnetization by two will lead to an immediate bounce and the loop will close. In practice this idea can be implemented by attempting to change the magnetization only by one, and accepting 50% of the attempts when the initial spin state is ± 1.

To study the efficiency of the new loop move, integrated autocorrelation times have been calculated. The normalized autocorrelation function is defined as,

$$A_Q(t) = \frac{\langle Q(i+t)Q(i)\rangle - \langle Q(i)\rangle^2}{\langle Q(i)^2\rangle - \langle Q(i)\rangle^2}, \qquad (16)$$

where i and t are measured in units of Monte Carlo steps, with one Monte Carlo step defined as one diagonal update and one loop update. The integrated autocorrelation time is defined according to

$$\tau_{\text{int}}[Q] = \frac{1}{2} + \sum_{t=1}^{\infty} A_Q(t). \qquad (17)$$

In Fig. 3 integrated autocorrelation times are shown for calculations using the old and the new loop updating method. The calculations are done on a system consisting of 32 spins without any disorder in the coupling
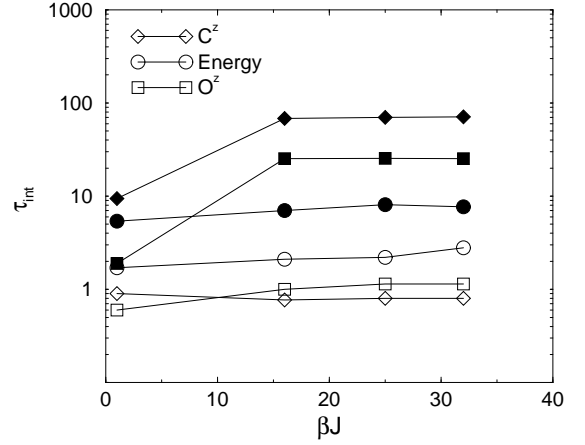

FIG. 3: Integrated autocorrelation times as a function of inverse temperature, βJ, for a system with 32 spins without bond disorder. The open symbols represents the directed loop updating method, where bounces have been excluded and the solid symbols are calculated using the original loop move.

parameters. The autocorrelation times are calculated for the energy and for the spin- and string-correlation function, which we now define.

The spin-correlation function $C^z(N)$ for a chain with N spins is measured at the greatest distance between two spins, which for periodic boundary conditions equals $N/2$,

$$C^z(N) = \frac{1}{N}\sum_{i=1}^{N}\langle S_i^z S_{i+\frac{N}{2}}^z\rangle, \qquad (18)$$

and the string-correlation function $O^z(N)$ is similarly defined by,

$$O^z(N) = \quad \frac{1}{N}\sum_{i=1}^{N}\langle S_i^z \exp[i\pi(S_{i+1}^z + S_{i+2}^z + \cdots \\ + S_{i+\frac{N}{2}-1}^z)]S_{i+\frac{N}{2}}^z\rangle. \qquad (19)$$

The energy is calculated according to[19]

$$E = -\frac{1}{\beta}\langle n\rangle, \qquad (20)$$

where n is the number of non-unit operators in the operator string. The energy autocorrelation time is least affected by the new loop update, as is clearly seen in Fig. 3. The reason is that the energy is not directly dependent on the loop move, since the energy is given by the number of operators which is determined in the diagonal update. The exclusion of the bounce shortens the autocorrelation time by up to two orders of magnitude for the spin correlation at low temperatures.

IV. DETERMINING AVERAGE AND TYPICAL CORRELATIONS

To calculate ground state expectation values in strongly disordered systems using QMC is not an easy task. The standard deviation in the disorder averaged expectation values has two sources: the standard statistical fluctuations, and the sample to sample variation. In strongly disordered systems the latter is often dominant and it is therefore advantageous to perform short simulations of a large number of disorder configurations. This is problematic for two reasons. First, each sample requires an adequate equilibration time, which becomes a very significant part of the simulation, particularly for short simulations. Second, it may be hard to determine at what temperature the expectation values have converged to their ground state values. Repeating the calculations at many temperatures is very time demanding.

Recently, a technique was proposed to alleviate these difficulties.[20] The basic idea is to perform a very small number of Monte Carlo steps at a series of decreasing temperatures. The method builds on two realizations. First, given an equilibrium Monte Carlo configuration at inverse temperature β it is possible to construct an approximate equilibrium configuration at inverse temperature 2β. Second, due to the extremely short autocorrelation times equilibrium is reached quickly. Due to the small number of Monte Carlo steps necessary at each temperature the methods allows very rapid calculation of disorder averages down to very low temperatures.

Now we will briefly describe the implementation of the method. The energy expectation value, see Eq. (20), is proportional to the length of the operator string and the temperature. This means that the length of the operator string is proportional to the inverse temperature β as the ground state is approached. The calculation begins at a high temperature, where a few equilibration Monte Carlo steps are performed, followed by a few steps when measurements are carried out. Thereafter the temperature is halved at the same time as the operator string is doubled. The procedure is repeated and results in a series of measurements at decreasing temperatures. This is carried on until disorder averages of the expectation values show no further temperature dependence.

In the random-singlet phase the spin-correlation functions have a very broad distribution. The average of the correlation functions will be dominated by very strong correlations, while the typical correlations are much weaker. In order to characterize this behavior we measure not only the average of the correlation function, but also the average of the logarithm of the correlation function, which defines the typical correlation function,

$$\log C_{\text{typ}}^z(N) = \frac{1}{N} \sum_{i=1}^{N} \log \langle S_i^z S_{i+\frac{N}{2}}^z \rangle. \tag{21}$$

The method described above is suitable for determining average correlation functions. However, it cannot be used to accurately determine typical correlation functions. The reason is that small values of the correlation functions give large contributions to the typical correlations. Therefore, the whole distribution of the correlation function needs to be determined quite accurately to investigate the typical behavior. In the above method the statistical errors for a single disorder configuration are very large, due to the small number of Monte Carlo steps. Hence the weak correlations, which are important for the typical correlations, drown in the statistical noise. In particular, many negative values will have to be discarded since the logarithm is defined only for positive arguments. In order to determine typical correlation functions we have therefore done the simulation in two stages. First we use the above method to determine the temperature at which average correlation functions have converged in temperature. Thereafter we perform much longer simulations at this temperature to determine the typical correlation functions.

V. RESULTS FOR THE RANDOM-BOND CHAIN

The properties of the random-singlet phase are predicted to be independent of the underlying Hamiltonian, as long as the ground state of two nearest-neighbor spins is a singlet. In particular, the decay exponents of the spin and string-correlation functions should be the same for the spin-1 and spin-1/2 chain.[10] In the random-singlet phase it is predicted that the average correlation functions decay algebraically,[4]

$$C^z(N) \propto N^{-2} \tag{22}$$

for large N, and

$$O^z(N) \propto N^{-\frac{3-\sqrt{5}}{2}} \simeq N^{-0.382}, \tag{23}$$

while typical correlations decay with a stretched exponential as

$$C_{typ}^z(N) \propto \exp(-A\sqrt{N}), \tag{24}$$

where A is a non-universal constant.

To make sure that the QMC method is capable of correctly determining the correlation functions for a strongly disordered spin system we have first performed a calculation on the spin-1/2 XX chain with bond disorder. The XX chain is described by the following Hamiltonian,

$$H = \sum_i J_i(S_i^x S_{i+1}^x + S_i^y S_{i+1}^y), \tag{25}$$

where $\mathbf{S}$ denotes a spin-1/2 operator. The ground state expectation values of the correlation functions for this system have been calculated by exact diagonalization using the Jordan-Wigner transformation to free fermions.[8] We compare QMC results for the average correlation
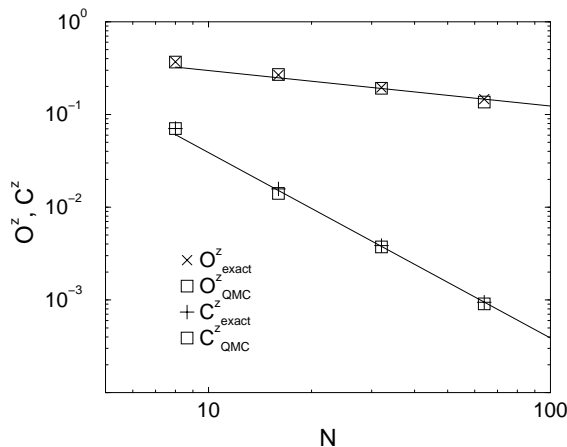
FIG. 4: A comparison between exact diagonalization and QMC results for the correlation functions of the spin-1/2 XX chain with bond disorder. Lines show algebraic decay with exponents predicted from RG calculations. The lines are drawn through the last exact diagonalization data point.
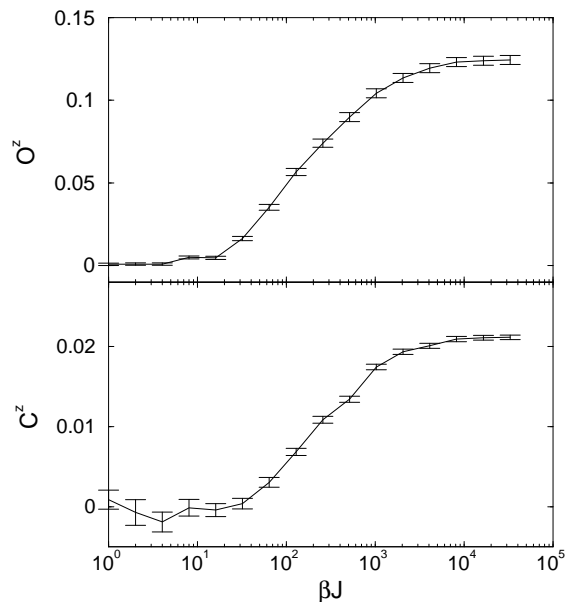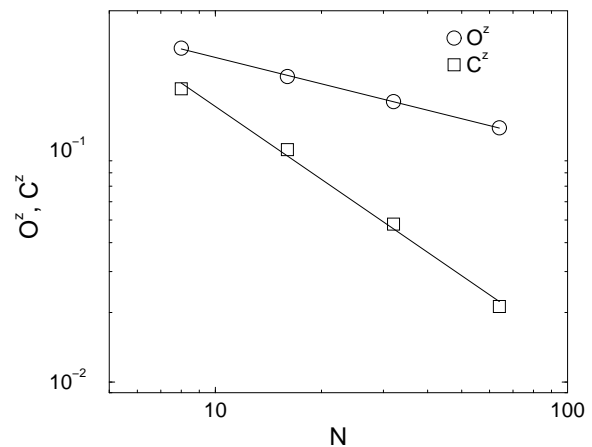

FIG. 6: The spin- and string-correlation functions for the bond-disordered spin-1 chain. Disorder averages are taken over at least 1000 configurations. The solid lines are linear fits to the data points.

FIG. 5: The temperature dependence of the string- and spin-correlation function for a system with 64 spins.

functions with the diagonalization data in Fig. 4 and there is very good agreement. The lines are drawn through the last diagonalization data point with the predicted slopes of -2 for the spin-correlation function and -0.382 for the string-correlation function. We can see that already for these relatively small system sizes the data displays almost linear behavior with slopes close to the predicted values. The finite-size corrections are more pronounced for the string-correlation function.

Next we consider the spin-1 chain. Recent numerical studies of the disordered spin-1 chain have used bonds

distributed according to a box distribution

$$P(J) = \begin{cases} 1/W & \text{for } 1 - \frac{W}{2} \le J_i \le 1 + \frac{W}{2} \\ 0 & \text{otherwise.} \end{cases} \qquad (26)$$

A density matrix renormalization group study did not find a transition to the random-singlet phase,[11] even for the strongest disorder ($W = 2$), while a QMC study[13] found evidence for a transition around $W = 1.8 - 1.9$. According to the RG analysis by Hyman and Yang[12] the phase transition occurs for the power law distribution, $P(J) \propto J^{-0.33}$, which represents stronger disorder than the box distribution. Finally, a recent RG study[14] finds that the transition occurs exactly at $W = 2$. Close to the critical point the RG studies find that the Haldane phase is Griffiths-like, with no gap, finite string order and exponentially decaying spin-correlation functions.

In this work we do not attempt to find the critical bond distribution. Instead we try to resolve the controversy concerning the box distribution. We focus on the widest possible box distribution and make an extensive QMC simulation of the correlation functions to determine whether they behave according to the random-singlet predictions.

The temperature dependence of the average string- and spin-correlation function for system size $N = 64$ is shown in Fig. 5. At each temperature we performed 20 equilibration steps followed by 60 measurement steps. The results seem to have converged (within statistical error bars) at approximately $\beta \approx 32000$. The convergence temperatures for different system sizes are presented in Table I. At least 1000 disorder distributions are used in the calculations. For these system sizes the convergence temperature is given by $\beta = N^3/8$.

In the second stage of the simulations 10^3 calibration steps are done, followed by at least 2×10^3 measuring
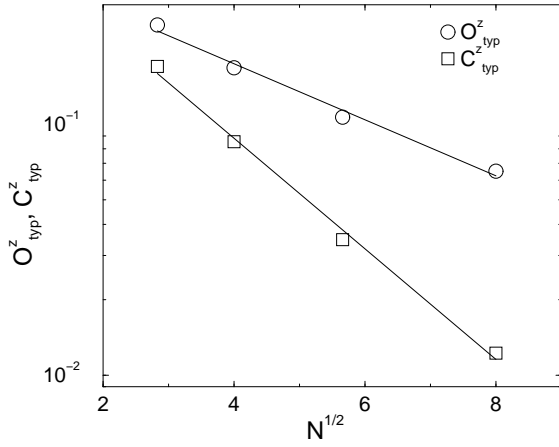
FIG. 7: The typical spin- and string-correlation functions as a function of the square root of the distance. The solid lines are linear fits to the data points.
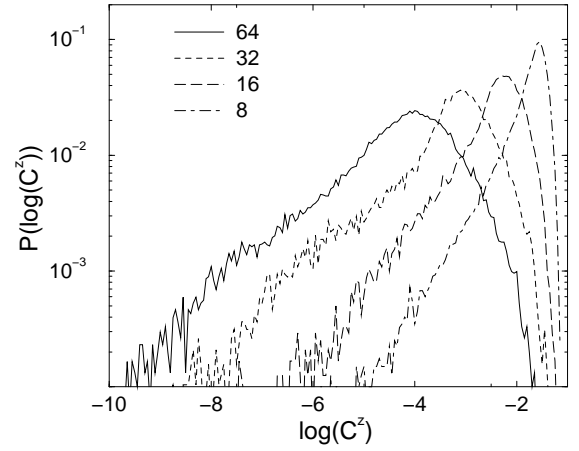

FIG. 8: Distribution of the spin-correlation function.

FIG. 9: The scaled distribution function for the spin-correlation function.

steps. Averages are calculated over 1000 disorder configurations. Results for average and typical correlation functions are shown in Fig. 6 and Fig. 7 respectively.

Straight lines are adjusted to the data points to determine the decay exponents in Fig. 6. In the log-log plot the string-correlation function displays very linear behavior, indicating that the function does decay algebraically. The decay exponent is found to be -0.378(6), in excellent agreement with the random-singlet prediction of -0.382. The spin-correlation function does not adjust to a straight line as well as the string correlation. The gradient of the curve increases with increasing system size. If a line is adjusted it results in a decay exponent of about -1.04(1), quite different from the predicted value of -2. The curvature of the function does indicates that we cannot see the true decay exponent with the limited system sizes used, and we cannot rule out the possibility that the exponent will converge to -2 for much larger system sizes. It is, however, remarkable that the spin-correlation function should display such dramatic system size dependence while the string-correlation functions has converged.

Next we consider the behavior of the typical correlation functions in Fig. 7. Straight lines should result if we plot the logarithm of the typical correlation functions versus the square root of the systems size. The QMC

System size	Inverse temperatures βJ
8	64
16	512
32	4096
64	32768

TABLE I: Inverse temperatures needed to reach ground state properties for different system sizes.

data lies close to a straight line, but there does seem to be a slight systematic curvature upwards. This can be explained by the difficulties in measuring the typical functions. A small percentage of the measurements are discarded since they are negative and this will result in too large an estimate. Since more points are dropped for the larger system sizes this should result in an upward curvature. For the 32-site system about 0.1 % of the points were dropped, while about 0.6 % of the points were dropped for the 64-site system. We believe that this explains the slight systematic deviation from the straight line.

We also considered the distribution of the correlation functions. According to the RG predictions the distribution of

$$\frac{\log\langle S_i^z S_{i+\frac{N}{2}}^z \rangle}{N^{\frac{1}{\mu}}} \qquad (27)$$

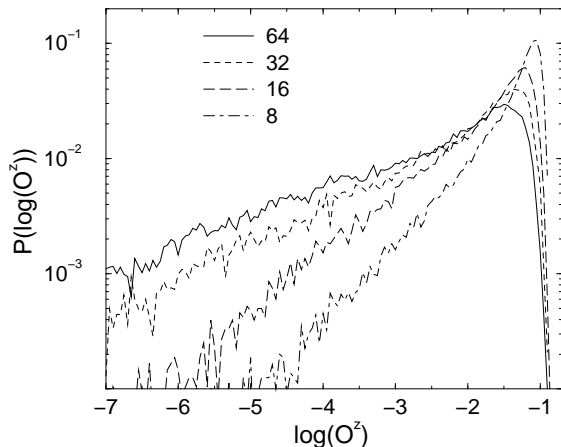should scale to a fixed distribution with $\mu = 2$. In Fig. 8

FIG. 10: Distribution of the string-correlation function.

we show the distribution of the logarithm of the spin-correlation function. The distribution becomes broader and the peak shifts to the left with increasing N. The best scaling plot was obtained with $\mu = 2.2$, shown in Fig. 9. The agreement with the RG predictions is again very good, but we were not able to scale the distribution of the string-correlation function. In Fig. 10 the unscaled distribution is shown, and as can be seen the distribution does broaden with increasing N, but much less than for the spin correlation function. In order to scale the distribution so that the peaks line up, a large value of $\mu \approx 10$ is needed, but then the rest of the distribution does not scale well.

Finally, we also studied the distribution of the local susceptibility,

$$\chi_{\text{loc}} = \frac{1}{N} \sum_i^N \int_0^\beta d\tau \langle S_i^z(0) S_i^z(\tau) \rangle, \qquad (28)$$

which is also predicted to scale according to Eq. (27). In agreement with the earlier QMC study performed at higher temperatures we also obtain the best scaling for $\mu = 2.5$.

VI. SUMMARY AND DISCUSSION

We have done extensive QMC simulations of the antiferromagnetic spin-1 Heisenberg chain with a uniform bond distribution extending all the way to zero bond strength. The calculations were performed at a temperature low enough for all observables to obtain their ground state expectation values. The decay exponent for the string-correlation function, as well as the typical correlation functions, are in good agreement with renormalization group predictions for the random-singlet phase. Our results for the average spin correlation function yields an exponent of -1.04(1) which differs significantly from

the RG prediction of -2. However, this result has not converged, but does display some finite-size effects. The distribution of the spin-correlation function is well described by RG predictions, but the distribution of the string-correlation function did not scale as predicted.

The very clear algebraic decay of the string order strongly indicates that the system in no longer in the Haldane phase. The exponent we obtained (-0.378(6)) is in excellent agreement with the prediction for the random-singlet phase (-0.382), and very different from the prediction[10] for the critical point separating the random singlet phase from the Haldane phase (-2/3). We therefore believe that our results are in agreement with earlier Monte Carlo results[13] and a recent RG calculation[14] showing that the box distribution extending all the way to zero is enough to drive the system to an infinite-randomness fixed point. The deviations from the random-singlet predictions could be explained by strong finite-size corrections. An alternative scenario is that the strong randomness fixed point for the spin-1 chain has slightly different properties from the spin-1/2 random-singlet fixed point.

To numerically determine the properties of the random-singlet phase for the strongly disordered spin-1 chain is much harder than for the spin-1/2 chain since a strong, finite disorder is needed to drive the chain to the random-singlet phase, according to the RG predictions. Disagreement between earlier numerical studies indicate the difficulties. The widest box distribution is expected to be quite close to the transition to the Haldane state, and it is possible that strong finite-size corrections appear in certain quantities. It would therefore be of great interest to study larger systems with even stronger, power-law distribution of the bonds. This is unfortunately not an easy task to do numerically. Density matrix renormalization group calculations yield ground state expectation values, but the method is most accurate for open boundary conditions for which finite size effects are stronger. Furthermore, it is hard to keep enough states to obtain accurate results for large systems with strong bond disorder. Using loop quantum Monte Carlo algorithms it is possible to reach fairly large system sizes at quite low temperatures, but to reach temperatures low enough to accurately determine the decay of correlation functions makes the simulations very time consuming. Furthermore, the expectation value of the correlation function becomes very small for large system sizes and long simulations are needed in order to reduce the statistical errors to the required level.

In conclusion, we believe that our results support earlier Monte Carlo simulations[13] and a recent RG calculation[14] indicating that the box distribution extending all the way to zero is wide enough to reach the random-singlet phase. With our present data we are not able to determine whether observed deviations from predictions for the random-singlet fixed point, most notably in the decay of the spin-correlation function, are due to strong finite-size corrections or slightly different

properties of the spin-1 random-singlet fixed point. To resolve this issue requires significant computational efforts and we leave it for future investigations. To obtain the present results we have implemented the concept of directed loops for the spin-1 chain and demonstrate that autocorrelation times are decreased by up to two orders of magnitude.

Acknowledgments

[*] Electronic address: sara@theophys.kth.se
[1] For reviews of quantum spin chains, see, e.g. A. Auerbach, *Interacting Electrons and Quantum Magnetism* (Springer Verlag New York, 1994); E. Fradkin, *Field Theories of Condensed Matter Systems* (Addison-Wesley 1991).
[2] S. R. White, Phys. Rev. Lett. **69**, 2863 (1992).
[3] S.-K. Ma, C. Dasgupta, and C.-K. Hu, Phys. Rev. Lett. **43**, 1434 (1979).
[4] D. Fisher, Phys. Rev. B. **50**, 3799 (1994).
[5] A. P. Young and H. Rieger, Phys. Rev. B **53**, 8486 (1996).
[6] K. Hida, J. Phys. Soc. Jpn. **65**, 895 (1996).
[7] A. Juozapavîcius, S. Caprara, and A. Rosengren, Phys. Rev. B **56**, 11097 (1997).
[8] P. Henelius and S. M. Girvin, Phys. Rev. B **57**, 11457 (1998).
[9] F. D. M. Haldane, Phys. Rev. Lett. **93A**, 464 (1983).
[10] R. A. Hyman and K. Yang, Phys. Rev. Lett. **78**, 1783 (1997).
[11] K. Hida, Phys. Rev. Lett. **83**, 3297 (1999).
[12] R. A. Hyman and K. Yang, Phys. Rev. Lett. **84**, 2044 (2000).
[13] S. Todo, K. Kato, and H. Takayama, J. Phys. Soc. Jpn. **69**, 355 (2000).
[14] A. Saguia, B. Boechat, and M. A. Continentino, cond-mat/0205492.
[15] A. W. Sandvik, Phys. Rev. B **59**, R14157 (1999).
[16] O. F. Syljuåsen and A. Sandvik, condmat/0202316.
[17] P. Henelius, P. Fröbrich, P. J. Kuntz, C. Timm, and P. J. Jensen, condmat/0204629.
[18] K. Harara and N. Kawashima, condmat/0205472.
[19] A. W. Sandvik, J. Phys. A **25**, 3667 (1992).
[20] A. W. Sandvik, condmat/0110510.